Biochemical and Biophysical Research Communications **290,** 113–120 (2002)
doi:10.1006/bbrc.2001.6190, available online at http://www.idealibrary.com on IDEAL®

FGFR3 Isoforms Have Distinct Functions in the Regulation of Growth and Cell Morphology

Akio Shimizu, Yuji Takashima, and Misuzu Kurokawa-Seo[1]
Department of Biotechnology, Faculty of Engineering, Kyoto Sangyo University, Kamigamo-Motoyama, Kita-ku, Kyoto 603-8555, Japan

Received November 19, 2001

We have previously cloned the alternatively spliced isoform of fibroblast growth factor receptor 3 (FGFR3ΔAB) that lacks the acid box in the extracellular region. To understand the biological functions and signal transduction of these FGFR3 isoforms, we analyzed the effect of FGF1 in ATDC5 cells, chondroprogenitor cell lines overexpressing these isoforms. In response to FGF1, FGFR3 induced a marked cell-morphology change to a round shape, while FGFR3ΔAB did not. Furthermore, FGFR3 induced complete growth arrest, whereas FGFR3ΔAB induced only moderate growth inhibition. Both receptors induced the expression of the CDK inhibitor $p21^{CIP1}$. However, only FGFR3 induced STAT1 phosphorylation that mediates the transcriptional induction of $p21^{CIP1}$, although both FGFR3 isoforms could induce a strong activation of mitogen-activated protein (MAP) kinases. Taken together, the different biological responses mediated by FGFR3 and FGFR3ΔAB appear to be due to a difference in their ability to utilize STAT1 pathway and signals involved in cell rounding. © 2002 Elsevier Science

Key Words: **cell rounding; STAT1; $p21^{CIP1}$; MAP kinases.**

Biochemical and genetic studies have shown that fibroblast growth factors (FGFs) and FGF receptors (FGFRs) play key roles in chondrogenesis (1, 2). However, FGFR3 is a negative regulator of chondrocytes, in contrast to the usual role of FGFRs, which are associated with increased cell proliferation (3). The role of FGFR3 in growth inhibition is cell-type specific, whereby the receptors utilize a signal pathway through STAT1 activation. Ligand stimulation of FGFR3 in a rat chondrosarcoma cell line and the thanatophoric dysplasia type II (TDII) mutant (K650E) of FGFR3 expressed in 293 cells increases the phosphorylation of STAT1 and its translocation to the nucleus. Activated STAT1 functions as a transcription factor to induce the expression of the cyclin-dependent kinases (CDK) inhibitor $p21^{CIP1}$ (4–6). This inhibits both the cyclin D-cdk4 and cyclin E-cdk2 complexes, thereby eliciting growth arrest in chondrocytes. However, the molecular basis for such signaling mediated by FGFR3 is not well defined.

The FGFR family consists of four members with related structures that have three different parts: an extracellular portion with three immunoglobulin-like (Ig) domains, a single transmembrane portion, a split tyrosine-kinase domain inside the cell (7). Alternative splicing of each FGFR transcript generates additional receptor isoforms with novel ligand affinities and unknown signaling cascades (7–11). In the segment of the extracellular domain between the first Ig (IgI) and the second Ig (IgII), there is a cluster of acidic residues, which is referred to as an "acid box" (7, 11, 12). We have previously identified an alternatively spliced isoform of FGFR3, designated as FGFR3ΔAB that lacks this acid box (14). We have also determined that the gene expressions of FGFR3 and FGFR3ΔAB were regulated differently during chondrogenic differentiation. However, the biological function these FGFR3 isoforms serve in chondrogenesis has not yet been determined.

In this study, we have addressed the role of FGFR3 isoforms in the growth inhibition of ATDC5 cells in response to FGF1 stimulation. ATDC5 cells are a murine chondroprogenitor cell line, which is undifferentiated and undergoes chondrogenesis in successive steps *in vitro* (15). In this report, we show that FGF1 inhibits cell growth in undifferentiated ATDC5 cells stably expressing FGFR3 and FGFR3ΔAB. The growth inhibition mediated by these isoforms is likely to be due to the induction of the $p21^{CIP1}$ protein expression. However, activation of FGFR3 phosphorylated STAT1 and elicited a marked morphological change to a round shape and detachment from the substratum, while FGFR3ΔAB induced neither response.

[1] To whom correspondence and reprint requests should be addressed. Fax: +81-75-705-1893. E-mail: mseo@cc.kyoto-su.ac.jp.

0006-291X/02 $35.00
© 2002 Elsevier Science
All rights reserved.

MATERIALS AND METHODS

Materials. Human recombinant FGF1 was purchased from R&D Systems (Minneapolis, MN). Heparin (Hepar Inc.) was a gift from Dr. J. Folkman. ATDC5 cells were kindly provided by Dr. Y. Hiraki, Japan.

FGFR expression plasmids and stable expression. Full-length cDNAs encoding the FGFR3ΔAB and FGFR3 were cloned into the pBKRSV expression vector (Stratagene, La Jolla, CA), as described previously (14). To express these FGFRs in ATDC5 cells, 4×10^6 cells were incubated with 20–30 μg of pBKRSV-FGFR3 or pBKRSV-FGFR3ΔAB plasmids for 10 min at 4°C. The ATDC5 cells were then electroporated in a Bio-Rad Gene pulser at 400 V and 960 μF before being plated. After 2–3 days of incubation in a maintenance medium containing 5% FBS, the ATDC5 cells were recovered. After washing with the medium, the ATDC5 cells were selected with 400 μg/ml G418 for 2 weeks.

Cell culture. ATDC5 cells were cultured in a maintenance medium consisting of a 1:1 mixture of Dulbecco's modified Eagle and Ham's F-12 medium (Life Technologies, Inc.) containing 5% FBS (JRH Biosciences Co. Lenexa, KS), 10 μg/ml bovine transferrin (Sigma), and 3×10^{-8} M sodium selenite (Sigma), as described previously (14). Cells were maintained at 37°C in a humidified 5% CO_2, 95% air atmosphere. The inoculum size of the cells was 6×10^3 cells/well in a 24-multiwell plate and 2.5×10^5 cells/plate in a 100-mm plate (Becton–Dickinson Labware).

Isolation of plasma membranes. Subconfluent dishes of ATDC5 cell lines (three 15-cm plates, approximately 1.1×10^7 cells) were rinsed with ice-cold PBS, scraped from the dishes, and pelleted. Cells were homogenized in 5 ml of isotonic buffer containing 50 mM Hepes buffer, pH 8.0, 200 mM sucrose, 2 mM EDTA, and 1 mM phenylmethylsulfonyl fluoride (PMSF) with 20 strokes in a Potter–Elvehjem tissue homogenizer. After removing cell debris by low-speed centrifugation, the supernatant was centrifuged at 100,000*g* for 1 h at 4°C and the pellet was resuspended in 50 μl of RIPA buffer (50 mM Tris–HCl (pH 8.0), 150 mM NaCl, 0.1% SDS, 1% sodium deoxycholate, 1% Triton X-100, 1 mM Na_3VO_4, and 1 mM PMSF). Protein concentrations were determined using a DC protein microassay (Bio-Rad).

Preparation of cell lysates and immunoprecipitation. Cells were cultured both in the presence and absence of FGF1 and heparin during the indicated periods. The medium then was removed, and the cells washed twice with cold PBS, before being collected using a cell scraper, and transferred into a 1.5 ml microtube. Cells were lysed with cold RIPA buffer. Protein concentrations were determined using a DC protein microassay (Bio-Rad). The protein extracts (500 μg) were immunoprecipitated with specific antibodies overnight at 4°C, and following the addition of 10 μl of protein A–Sepharose (CL-4B, Amersham Pharmacia Biotech) the mixtures were incubated for 1 h at 4°C. The protein A–antibody–antigen complexes were washed four times with the RIPA buffer and separated on SDS–PAGE. For the cell lysates, an equal amount of protein (60 μg) was loaded in each gel lane.

Western blot analysis. Proteins were electrophoresed through SDS–7.5 or 12.5% acrylamide gels, and then transferred to PVDF membranes (Immobilon-P, Millipore Co.). After a 2 h incubation in blocking solution (5% nonfat dried milk in TBS), the protein blots were probed with primary rabbit or mouse antibodies for 1 h at room temperature and then with horseradish peroxidase-conjugated second antibody (Santa Cruz Biotechnology, Santa Cruz, CA). The blots were treated for 5 min using an enhanced chemiluminescence substrate solution (Super Signal West Pico, Pierce, Illinois) and exposed to BioMax MS film (Eastman Kodak Co.) to visualize immunoreactive bands. The primary antibodies used were: anti-C-terminal FGFR2 or FGFR3 antibody, anti-phosphotyrosine antibody PY20, anti-$p21^{CIP1}$ antibody (Santa Cruz Biotechnology), anti-phosphorylated MAPK antibody, anti-MAPK antibody (NEB), and anti-phosphorylated STAT-1 antibody (Upstate).

RNA extraction and RT-PCR analysis. ATDC5 cells were inoculated into 100-mm plates and cultured in the maintenance medium both with and without 10 ng/ml of FGF1 and 10 μg/ml of heparin for 2 days. Total RNA was prepared from the cultures using Isogen (Nippon Gene Co., Tokyo) following the instructions given by the supplier. The first strand of cDNA was synthesized using avian myeloblastosis virus reverse transcriptase (RNA kit; Takara) and PCR was performed as described previously (14). The optimal Mg^{2+} concentrations used were 2.5 mM for integrins and 1 mM for glyceraldehyde-3-phosphate dehydrogenase (GAPDH). The forward and reverse primers used were: α2 integrin; 5′-gat aaa gac acc att aca gac gtg-3′ and 5′-cac atc att aaa gcc atc cat gttg-3′, α5 integrin; 5′-ctg cag ctc cat ttc cga gtc tgg-3′ and 5′-gaa gcc gag ctt gta gag gac gta-3′, GAPDH; 5′-acc aca gtc cat gcc atc ac-3′ and 5′-tcc acc acc ctg ttg ctg ta-3′, respectively. The amounts of mRNA were adjusted in each RT-PCR by checking amplification of GAPDH transcripts. A linear amplification dependent on the amount of RNA was obtained under the above conditions (from 2.5 to 40 ng RNA). Aliquots of the PCR products (10 μl) were electrophoresed on 3.5% agarose gels (Nusieve GG/Seakem) in Tris acetate EDTA buffer, pH 8.0, and stained with 0.5 μg/ml ethidium bromide.

Cell growth assays. Cell proliferation was assayed by counting the number of ATDC5 cells stably expressing FGFR3ΔAB or FGFR3 or ATDC5 cells transfected with pBK-RSV. Cells were washed twice with a maintenance medium containing 5% FBS, and then plated at 6×10^3 per well in a total volume of 500 μl medium in 24-multiwell plates. On the next day, FGF1 (10 ng/ml) was added in the presence of 10 μg/ml heparin. On the days indicated the cells were trypsinized and counted with a Coulter Counter ZM type (Beckman Coulter Co.). Experiments were performed at least in triplicate and the results are expressed as means ± standard deviations.

RESULTS

FGFR3 isoforms induce distinct morphological responses in ATDC5 cells. To study the function of FGFR3 and FGFR3ΔAB (the isoform that lacks the acid box domain of FGFR3) in ATDC5 cells, we transfected ATDC5 cells with recombinant pBKRSV vectors encoding mouse FGFR3 or FGFR3ΔAB and selected representative clones. We analyzed the expression levels of FGFR3 isoforms in these clones (Fig. 1A). Although murine FGFR3 and FGFR3ΔAB cDNAs encode 800 and 782 residue proteins respectively (14), the bands corresponding to overexpressed FGFR3 and FGFR3ΔAB proteins were almost identical in size (apparent molecular mass of 140 kDa), and the empty vector-introduced ATDC5 cells expressed an endogenous FGFR3ΔAB protein (Fig. 1A). The difference between the expected masses of these receptors from the deduced amino acid residues (FGFR3; 88 kDa and FGFR3ΔAB; 86 kDa) and the apparent molecular mass is likely to be due to glycosylation of these receptors (16). In addition, vector-introduced ATDC5 cells and representative clones express high levels of FGFR2 isoforms (120 kDa and 140 kDa) endogenously (Fig. 1A). This agrees with an earlier study indicating that undifferentiated ATDC5 cells express a low level of FGFR3ΔAB and high levels of FGFR2 isoforms (14).

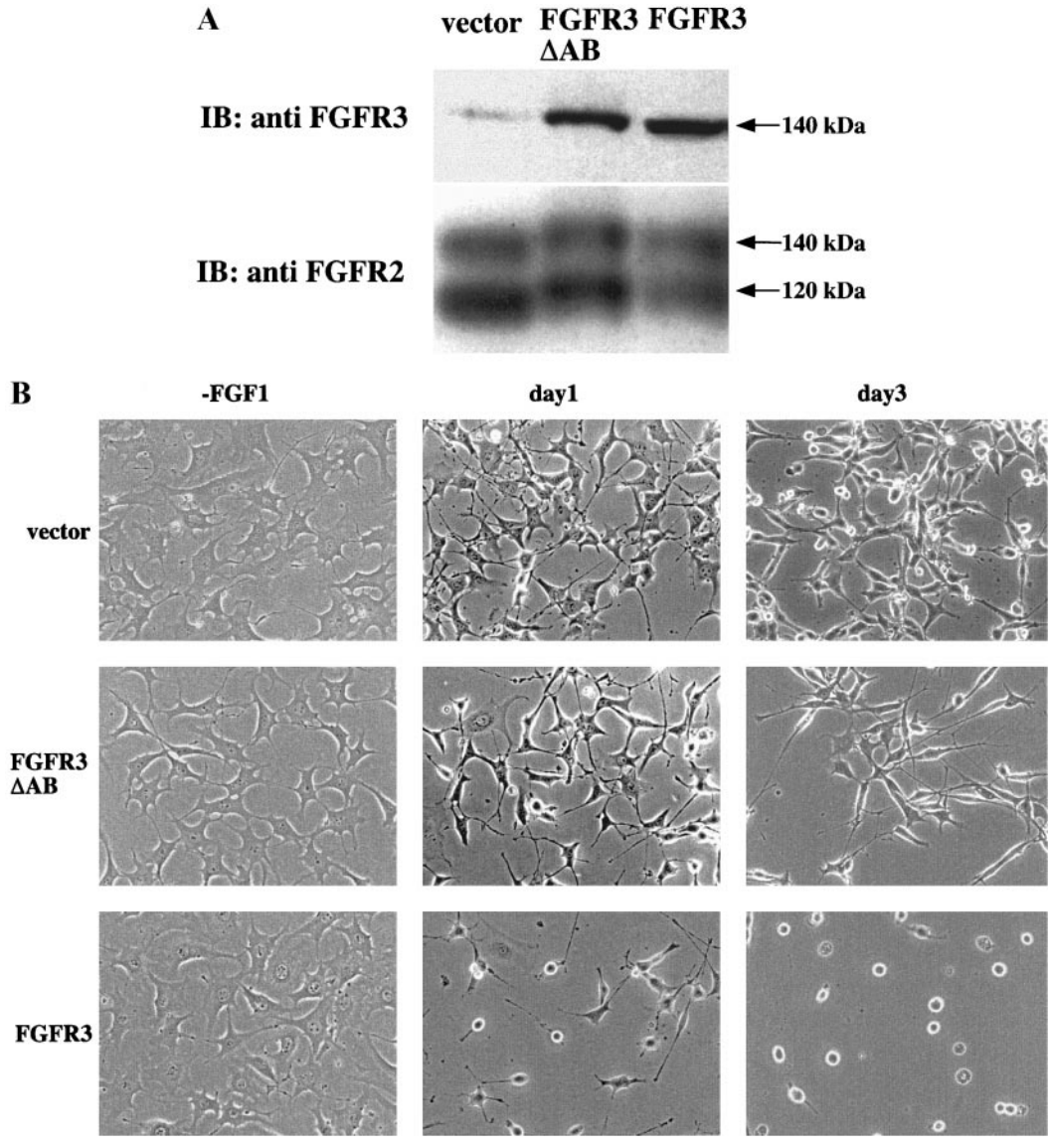

FIG. 1. FGFR3 induces cell rounding of ATDC5 cells in response to FGF1, but FGFR3ΔAB does not. (A) Western blot analysis of FGFR expression in ATDC5 cells. For each ATDC5 cell line, the cell membranes were prepared as described under Materials and Methods and 100 μg protein was analyzed in the Western blot. An antibody directed against the carboxyl terminus of FGFR3 FGFR2 or FGFR3 was used to visualize the receptor isoforms present in cell membranes. ATDC5 cells expressing FGFR3, (FGFR3); ATDC5 cells expressing FGFR3ΔAB, (FGFR3ΔAB); ATDC5 cells transfected with pBK-RSV vector alone, (vector). (B) FGFR3 expressing ATDC5 cells changed their morphology to a round shape and the cells became disengaged from the dish, whereas FGFR3ΔAB did not. ATDC5 cells were seeded at 2.5×10^5 cells in a 100-mm plate in DME/F-12 medium containing 5% FBS. The next day, 10 ng/ml of FGF1 and10 μg/ml of heparin were added and incubated for 1–3 days (day 1, day 3) or untreated (−FGF1).

We noticed marked differences in cell shape between cells expressing FGFR3 and those expressing FGFR3ΔAB, when these cells were treated with FGF1. In the absence of FGF1, these cells spread out and attach firmly to the substratum (Fig. 1B, −FGF1). In response to FGF1 stimulation, the morphology of the cells expressing FGFR3 started to change from a flattened shape to a round shape. Cells became disengaged from the dish and cell rounding was observed after one day's treatment with FGF1 (FGFR3, day 1) and finally showed complete cell rounding (FGFR3, day 3). On the other hand, C2 cells and ATDC5 cells expressing FGFR3ΔAB started to adopt a spindle-like shape after one day's treatment with FGF1 (vector, FGFR3ΔAB, day 1). After 3 days, ATDC5 cells expressing FGFR3ΔAB were longer than C2 cells (C2 and FGFR3ΔAB, day 3). Similar cell rounding was observed in other clones expressing FGFR3, whereas no clones expressing FGFR3ΔAB showed cell rounding even in the higher concentrations of FGF1 (data not shown). To test the relationship between the marked difference in FGF1-induced morphological changes in FGFR3 and

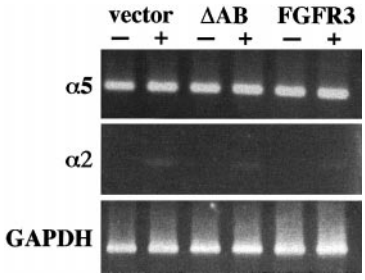

FIG. 2. RT-PCR analysis of $\alpha 2$ and $\alpha 5$ integrin expression in ATDC5 cells. ATDC5 cell lines expressing FGFR3 (FGFR3) or FGFR3ΔAB (ΔAB) and ATDC5 cells transfected with pBK-RSV alone (vector) were grown in a maintenance medium containing 5% FBS and treated with 10 ng/ml of FGF1 and10 μg/ml of heparin (+) or untreated (−). The total RNA was isolated after 2 days of culture. The RT-PCR was performed as described under Materials and Methods, using the primers for $\alpha 5$ integrin, $\alpha 2$ integrin or GAPDH.

FGFR3ΔAB clones and the decreased expression of integrins, we analyzed the gene expression of subunits $\alpha 5$ and $\alpha 2$ in response to FGF by RT-PCR (Fig. 2). Integrins are heterodimer adhesion molecules composed of α- and β- subunits (17). The interaction of $\alpha 5\beta 1$ integrin with fibronectin regulates proliferation of chondrocytes positively and is involved in cell adhesion and spreading (18). Proliferating chondrocytes in the proliferative zone in rabbit growth plate cartilage interact with fibronectin through $\alpha 5\beta 1$ heterodimers, whereas in the maturing zone after exiting cell cycle chondrocytes, they preferentially interact with collagen type II through $\alpha 2\beta 1$ heterodimers (18). Furthermore, in CFK2 chondrocytic cells, expression of FGFR3 with the G380R achondroplasia mutation inhibits cell-proliferation, suggesting that the mechanism of inhibition is related to altered integrin expression (19). However, as shown in Fig. 3, the gene expression of $\alpha 5$ integrin subunits was unchanged in all ATDC5 cell lines after one day of FGF1 treatment, at which time cell-rounding was induced in the cells expressing FGFR3. In contrast, FGF1 treatment weakly enhanced $\alpha 2$ integrin expression in all clones. These results indicate that the change to a round morphology in ATDC5 cells expressing FGFR3 was not due to a decrease in the expression of the fibronectin receptor. In addition, we have also examined the gene expression of collagen type II. Although FGF1 treatment induced a transient up-regulation of collagen type II transcripts in all clones including C2 cells, there was no appreciable difference between ATDC5 cells expressing FGFR3 and FGFR3ΔAB (data not shown). Taken together, the FGF-induced cell rounding in ATDC5 cells expressing FGFR3 is most likely due to regulation of the cytoskeletal organization rather than that of altered integrin expression. Further studies would be needed to prove this.

FGFR3 isoforms induce growth inhibition in ATDC5 cells. As shown in Fig. 1B, FGFR3 induced cell rounding in response to FGF1, whereas FGFR3ΔAB did not. Cell adhesion to extracellular matrix and associated changes in cell shape control cell growth and function (20). Therefore, FGFR3 may inhibit cell growth in ATDC5 cells by inducing cell rounding. To determine the effect of FGF1 on the growth of ATDC5 cells expressing FGFR3 or FGFR3ΔAB, we seeded 6,000 cells per well in a 24-multiwell plate and counted the numbers of these cloned cells after 4 days in culture in the absence or the presence of various concentrations of FGF1. Treatment with FGF1 strongly stimulated cell proliferation of ATDC5 cells transfected with the empty vector. As described previously, the endogenous expression of FGFR1 and FGFR2 in parent cells ATDC5 (14) is thought to be responsible for the stimulatory effect of FGF1 in the empty vector transfected cells. On the contrary, FGF1-treatment suppressed proliferation of the cells expressing FGFR3 or FGFR3ΔAB in a dose dependent manner (Fig. 3A). Interestingly, the growth of the FGFR3ΔAB clone was also strongly inhibited by FGF1 treatment, although cell rounding was not observed in the cells (Fig. 1B). The effects of FGF1 in growth inhibition in FGFR3ΔAB and FGFR3 clones were saturated at 313 pM concentration. At lower concentrations of FGF1, however, FGFR3 inhibited cell growth stronger than FGFR3ΔAB did. In Fig. 3B, growth rates of the empty vector-transfected cells and representative clones expressing FGFR3 and FGFR3ΔAB in the absence or the presence of the saturated concentration of FGF1 (10 ng/ml, 645 pM) were shown. Growth suppression in both FGFR3 and FGFR3ΔAB cells was evident by day 3. In the presence of FGF1, FGFR3 induced complete arrest of cell growth, whereas FGFR3ΔAB induced growth suppression but not complete arrest. The effect of FGF1 lasted for 8 days, although it was added only once to the medium on day 1. Even in the absence of FGF1, the clone expressing FGFR3 showed a slower growth rate compared to other clones. This may be due to the endogenous expression of FGF1 and FGF2 in ATDC5 cells. Thus, we also tested growth rates of the other clones expressing FGFR3 and these showed also slower growth rates in the absence of FGF1 (data not shown). These results demonstrate that, in response to FGF1, FGFR3 and FGFR3ΔAB mediate signals eliciting growth inhibition in ATDC5 cells, even if the cells are not differentiated to chondrocytes.

FGFR3ΔAB is not able to utilize the STAT1 signaling pathway for induction of the CDK inhibitor $p21^{CIP1}$. The $p21^{CIP1}$ protein inhibits cyclin-dependent kinase (CDK) activity that is essential for cell cycle progression from the G1-phase to the S-phase (21). In chondrocytes, FGFR3 signaling induces up-regulation of $p21^{CIP1}$ and eventually causes growth arrest (4–6). To

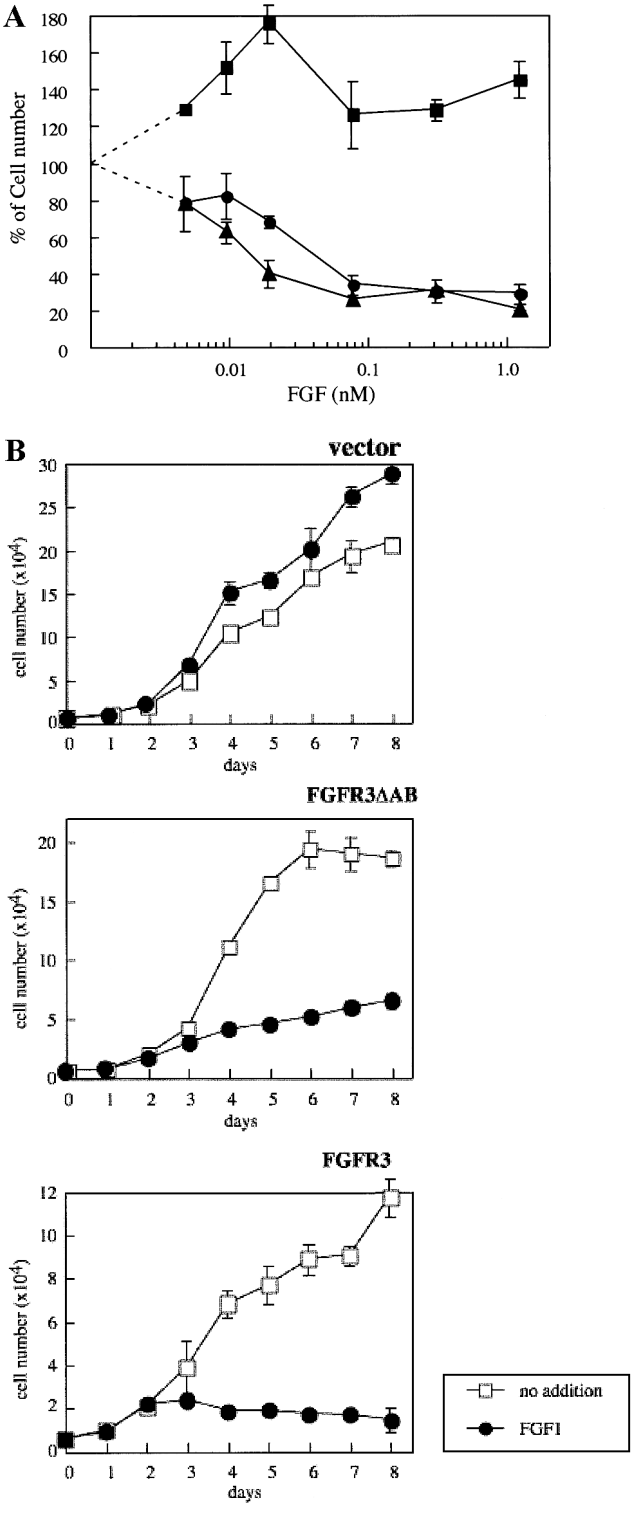

FIG. 3. FGFR3 and FGFR3ΔAB induce growth inhibition in ATDC5 cells. (A) Effects of FGF1 concentrations. ATDC5 cells were seeded at 6×10^3 cells/well in 24-multiwell plates in DME/F-12 medium containing 5% FBS. The next day (day 1), various concentrations of FGF1 as indicated on the graph and 10 μg/ml of heparin were added. On day 4, the number of cells per culture was measured with a Coulter counter (ZM) after collecting the cells with trypsin. Data are shown as % of cell number in the absence of FGF1 and obtained from triplicate experiments. The upper and lower panels show the high and the low concentration points of FGF1, respectively. ATDC5 cells expressing FGFR3 (FGFR3) or FGFR3ΔAB (FGFR3ΔAB), and ATDC5 cells transfected with pBK-RSV alone (vector). The cell number in the absence of FGF1 was: ATDC5 cells expressing FGFR3, 50,540 ± 7,354 (± SD). ATDC5 cells expressing FGFR3ΔAB; 110,393 ± 4,058. ATDC5 cells transfected with an empty vector; 103,840 ± 3,018. (B) Growth rates of vector transfected (vector), and derivative clones overexpressing FGFR3 or FGFR3ΔAB are shown in the absence or the presence of FGF1. ATDC5 cells were seeded at 6×10^3 cells/well in 24-multiwell plates in DME/F-12 medium containing 5% FBS. The next day (day 1), 10 ng/ml of FGF1 and 10 μg/ml of heparin were added to some cultures (FGF1) or not added (no addition). The cells were incubated for periods indicated on the graph. The number of cells per culture was determined with a Coulter counter (ZM) after collecting the cells with trypsin and represented the means ± standard deviations of three wells.

determine whether FGFR3 and FGFR3ΔAB induced increased expression of $p21^{CIP1}$ in ATDC5 cells, we analyzed protein expression by Western blotting. After one day of treatment with FGF1, the expression of $p21^{CIP1}$ was detected in ATDC5 cells expressing FGFR3 (FGFR3 cells) and FGFR3ΔAB (FGFR3ΔAB cells), whereas not in the empty vector cells (Fig. 4A). The level of $p21^{CIP1}$ in FGFR3 cells peaked on day 2 of FGF1 treatment, whereas that in FGFR3ΔAB cells decreased after one day. These data demonstrated that the increased levels of $p21^{CIP1}$ lasted longer in FGFR3 cells than in FGFR3ΔAB cells, and complete FGFR3 cell growth arrest was noted from day 3 to 8 day (Fig. 3B), even though the level of $p21^{CIP1}$ declined after 3 days in FGFR3 cells. On the other hand, in FGFR3ΔAB cells the transient expression of $p21^{CIP1}$ acted only to slow the growth rate, but not to completely arrest it (Fig. 3B).

To define the FGF1-induced growth inhibitory signals from FGFR3 and FGFR3ΔAB, the induction of STAT1 phosphorylation was examined in these cell lines (Fig. 4B). STAT1 activation mediated by FGFR3 has been reported to be responsible for the increased expression of $p21^{CIP1}$ protein in chondrocytes (4). Activated STAT1 proteins specifically recognized the conserved STAT1 responsive elements in the promoter of the gene encoding $p21^{CIP1}$ and regulated the induction of $p21^{CIP1}$ messenger RNA (5). In this study, phosphorylated STAT1 protein was detected in FGFR3 cells after a 5 min treatment with FGF1, but not in the empty vector or FGFR3ΔAB cells. These results show that FGFR3 mediates STAT1 phosphorylation in ATDC5 cells as it does in chondrocytes. In addition, these results indicate that it is not necessary for cells to be differentiated to chondrocytes for FGFR3 to mediate STATI signals and to induce $p21^{CIP1}$ protein expression. However, FGFR3ΔAB is not able to stimulate STAT1 phosphorylation, suggesting that there must be another signaling pathway by which FGFR3ΔAB mediates the induction of $p21^{CIP1}$ expression in response to FGF1.

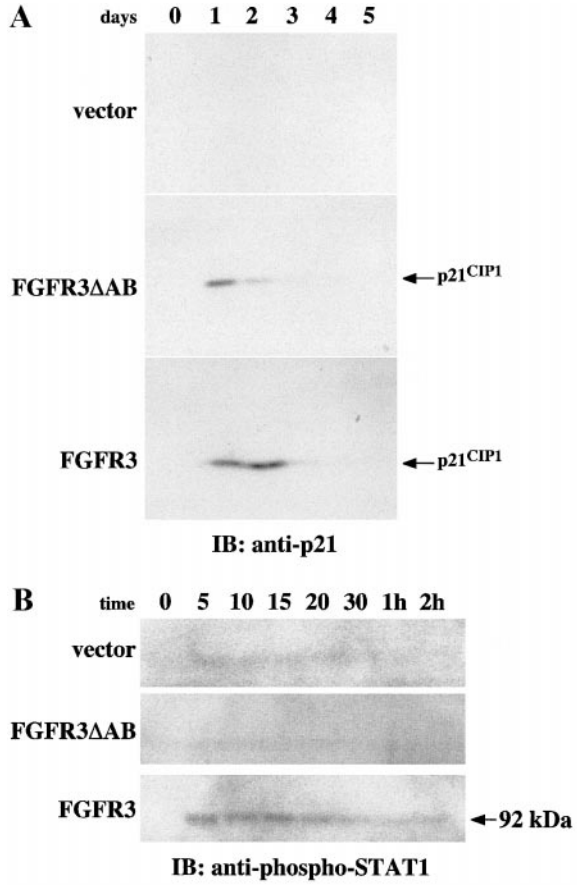

FIG. 4. Induction of the CDK inhibitor $p21^{Cip1}$ and activation of STAT1 in response to FGF1. (A) FGF1 treatment induces $p21^{Cip1}$ expression in ATDC5 cells expressing FGFR3 and FGFR3ΔAB. ATDC5 cells were grown in a maintenance medium containing 5% FBS and treated with 10 ng/ml FGF1 and 10 μg/ml heparin or untreated for the indicated (0–5) days. The cellular proteins were extracted with an RIPA buffer, and a total of 60 μg of protein was electrophoresed by SDS–PAGE before being analyzed by Western blot with an anti-p21 monoclonal antibody. (B) FGFR3 induced STAT1 phosphorylation in ATDC5 cells in response to FGF1, but FGFR3ΔAB did not. After treatment with FGF1 in the presence of heparin for the indicated times (5, 10, 15, 20, 30 min, 1 h, and 2 h) or untreated (0 min), cellular proteins were extracted with an RIPA buffer and a total of 30 μg of protein was electrophoresed before being analyzed with an anti-phosphorylated STAT1 antibody.

FGFR3 isoforms induce strong MAP kinase activation. The Ras/Raf/MAP kinase pathway can mediate a growth-promoting signal stimulated by FGFRs (22–24). Therefore, we investigated whether the growth-inhibitory effect of FGF1 on ATDC5 cells expressing FGFR3 isoforms was related to the MAP kinase pathway. As shown in Fig. 5A, FGF1 treatment of the empty vector cells induced phosphorylation of MAP kinases (ERK1; p44 and ERK2; p42) after as rapid as 5 min. Unexpectedly, phosphorylation of MAP kinases induced by FGF1 treatment was stronger in both FGFR3 and FGFR3ΔAB cells than in the empty vector cells. To assess activation of MAP kinases in those cells, phosphorylated MAP kinases were represented as a percentage of the total MAP kinases expressed in each cell line at the point in time when all cells were untreated (0 h) (Fig. 5B). In the empty vector cells, the maximal activation of MAP kinase was 45% after 10 min of treatment with FGF1, whereas in both FGFR3 and FGFR3ΔAB cells, it was over 65%. These results indicate that FGFR3 isoforms can mediate strong activation of MAP kinases, whereas in the empty vector cells, endogenous FGFRs can induce a moderate activation of MAP kinases.

DISCUSSION

Our experiments show that FGFR3 signals could induce cell rounding, whereas FGFR3ΔAB signals

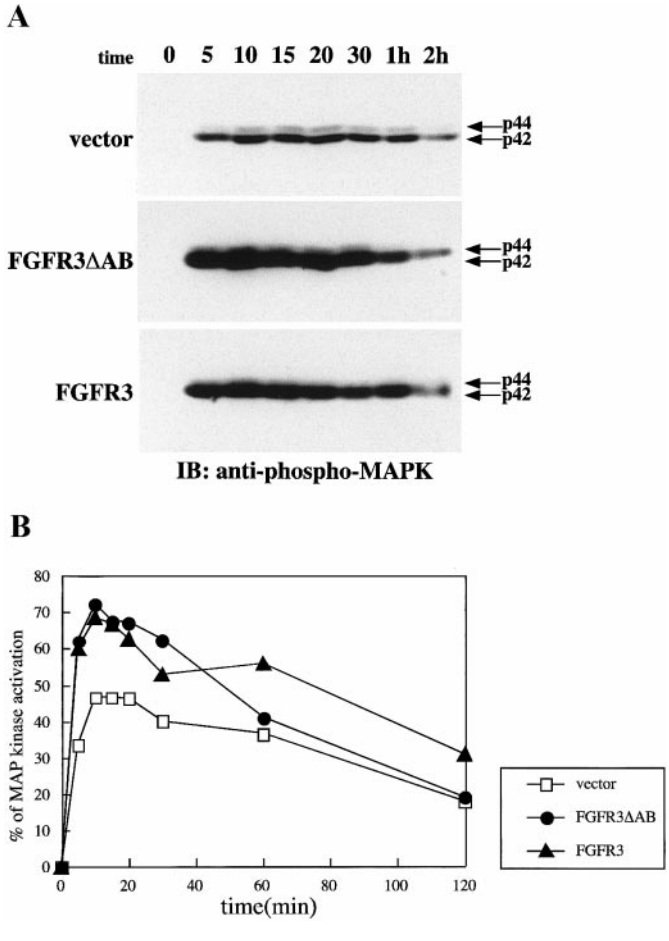

FIG. 5. Activation of MAP kinases in ATDC5 cells by FGFR3 and FGFR3ΔAB. (A) ATDC5 cells were treated with 10 ng/ml FGF1 and 10 μg/ml heparin for the indicated times (5, 10, 15, 20, 30 min, 1 h, and 2 h) or they were left untreated (0 min) as shown in Fig. 4B. Cell lysates (30 μg of protein) were analyzed directly by SDS–PAGE and immunoblotting with an anti-phosphorylated MAP kinase antibody. (B) Quantification of activated MAP kinase levels in FGF1-treated ATDC5 cells. Phosphorylated MAP kinases were represented as a percentage of the total MAP kinases expressed in each cell line at the point in time when all cells were untreated (0 h). Total MAP kinase proteins were detected after reprobing the same membrane with an anti-MAP kinase antibody.

could not (Fig. 1B). At the moment, we do not know how FGFR3 signaling in the cell causes reduced adhesion to the substratum and the morphological change to a round shape, since the gene expression of the fibronectin receptor subunit (α5 integrin) was unchanged after FGF1-treatment in FGFR3 cells. However, our results indicate that the acid box in the extracellular region of FGFR3 is required to mediate the signal for cell rounding. Recent studies have revealed the importance of adhesion-dependent control of cell-cycle progression (20, 25). Huang *et al.* hypothesized that cell shape is an important determinant in the progress of the cell cycle and that there is a cell shape-sensitive restriction point in late G1 (20). The anchorage-dependent G1 arrest has been attributed to increased levels of the CDK inhibitors $p27^{KIP1}$ and $p21^{CIP1}$, although the particular CDK inhibitor responsible varies in different studies (20). Therefore, FGFR3 may be able to strongly inhibit cell cycle progression in ATDC5 cells by inducing cell rounding. In addition, in FGFR3 cells, the increased level of $p21^{CIP1}$ induced by FGF1 could be maintained by the reduced adhesion to the substratum, thus allowing for complete growth arrest.

The mechanism by which FGFR3 transmits the growth inhibitory signal in chondrocytes has been thought to be the same one that activates STAT1 pathway leading to the transcriptional activation of $p21^{CIP1}$ (4–6). The binding of $p21^{CIP1}$ to cdk4 and cdk2 complexes inhibits cyclin D- and E-dependent kinase activities, thereby inhibiting cell cycle progression from the G1 to the S-phase (21, 26, 27). However, when FGFR3 was introduced into NIH3T3 cells, there was no STAT1 phosphorylation in response to FGF, and cell proliferation was stimulated (4). In addition, when FGFR3 was introduced into BaF3 cells, it also stimulated cell proliferation (14). These studies suggest that the activation of STAT1 and growth inhibition by FGFR3 may involve the specific cell environment of chondrocytes, where the receptor is capable of utilizing cell-type specific adaptor proteins that is absent from NIH3T3 cells and BaF3 cells (3, 4). If this is the case, our results demonstrate that undifferentiated ATDC5 cells also express the adaptor proteins and activation of FGFR3 leads to STAT1 phosphorylation. However, the mechanism by which FGFR3 can utilize a STAT1 pathway is still not proven. Furthermore, FGFR3ΔAB may be unable to use such adaptor proteins efficiently, in spite of the fact that the intracellular domain of the receptor is the same as FGFR3. Interestingly, although FGFR3ΔAB did not induce STAT1 phosphorylation in response to FGF1, the $p21^{CIP1}$ expression was elevated in FGFR3ΔAB cells after one day of FGF1-treatment (Fig. 4A). Hence, we thought there must be another signaling mechanism by which FGFR3ΔAB regulates the induction of $p21^{CIP1}$ expression in ATDC5 cells.

The Ras/Raf/MAP kinase (ERK) pathway has been shown to function in both the stimulation of cellular proliferation or the arrest of growth through induction of $p21^{CIP1}$ (26–28). The threshold of $p21^{CIP1}$ induction is the signal intensity of the MAP kinase pathway. A strong activation of MAP kinase elicits cell cycle arrest through the induction of $p21^{CIP1}$. Moderate activation of MAP kinase elicits a mitogenic response through the induction of cyclin D1, and a failure to induce $p21^{CIP1}$ expression in NIH3T3 cells (26, 27). Our results in ATDC5 cells may be consistent with this model. In other studies, strong activation of MAP kinase for only 1 h has been reported to induce significant biological responses such as the induction of $p21^{CIP1}$ and/or cell differentiation in HL60 cells and PC12 cells (29, 30). It seems likely, therefore, that in ATDC5 cells the strong activation of MAP kinase pathway is responsible for the $p21^{CIP1}$ induction mediated by FGFR3ΔAB (Fig. 4A). In addition, the difference in the levels of $p21^{CIP1}$ expression mediated by FGFR3 and FGFR3ΔAB appears to be due to a difference in their abilities to utilize the STAT1 pathway and may correlate with the extent of growth inhibition, e.g., complete growth arrest vs slower growth rate.

In a normal body, the timing of FGF signaling determined by regulation of receptor expression and alternative splicing is likely to be a critical factor in proper morphogenesis of cartilage and bone development. As previously shown in chondrogenesis *in vitro* using ATDC5 cells, the low level of FGFR3ΔAB expression may allow prechondrocytes and chondrocytes to finely regulate the growth rate in response to FGF signaling. In contrast, the increased expression of FGFR3 in chondrocytes completely induces growth arrest. Further studies are required to clarify the mechanism by which the acid box plays a role in FGFR3 signaling.

ACKNOWLEDGMENTS

We are grateful to Dr. T. Kurokawa for critical reading of the manuscript. We are also grateful to Mr. M. Nitta and Mr. N. Sato for helpful discussions.

REFERENCES

1. Naski, M. C., and Ornitz, D. M. (1998) FGF signaling in skeletal development. *Front. Biosci.,* 781–794.
2. Xu, X., Weinstein, M., Li, C., and Deng, C-X. (1999) Fibroblast growth factor receptors (FGFRs) and their roles in limb development. *Cell Tissue Res.* **296,** 33–43.
3. Kannan, K., and Givol, D. (2000) FGF receptor mutations: Dimerization syndromes, cell growth suppression, and animal models. *IUBMB Life* **49,** 197–205.
4. Sahni, M., Ambrosetti, D. C., Mansukhani, A., Gertner, R., Levy, D., and Basilico, C. (1999) FGF signaling inhibits chondrocyte proliferation and regulates bone development through the STAT-1 pathway. *Genes Dev.* **13,** 1361–1366.
5. Su, W. C., Kitagawa, M., Xue, N., Xie, B., Garofalo, S., Cho, J., Deng, C., Horton, W. A., and Fu, Z. Y. (1997) Activation of Stat1

by mutant fibroblast growth-factor receptor in thanatophoric dysplasia type II dwarfism. *Nature* **386,** 288–292.

6. Chin, Y. E., Kitagawa, M., Su, W. C. S., You, Z. H., Iwamoto, Y., and Fu, X. Y. (1996) Cell growth arrest and induction of cyclin-dependent kinase inhibitor p21 WAF1/CIP1 mediated by STAT1. *Science* **272,** 719–722.
7. Johnson, D. E., and Williams, L. T. (1993) Structural and functional diversity in the FGF receptor multigene family. *Adv. Cancer Res.* **60,** 1–41.
8. Xu, J., Nakamura, M., Crabb, J. W., Shi, E., Matuo, Y., Fraser, M., Kan, M., Hou, J., and McKeehan, W. L. (1992) Expression and immunochemical analysis of rat and human fibroblast growth factor receptor (flg) isoforms. *J. Biol. Chem.* **267,** 17792–17803.
9. Wang, F., Kan, M., Yan, G., and McKeehan, W. L. (1995) Ligand-specific structural domains in the fibroblast growth factor receptor. *J. Biol. Chem.* **270,** 10222–10230.
10. Ornitz, D. M., Xu, J., Colvin, J. S., McEwen, D. G., MacArthur, C. A., Coulier, F., Gao, G., and Goldfarb, M. (1996) Receptor specificity of the fibroblast growth factor family. *J. Biol. Chem.* **271,** 15292–15297.
11. Lopez, M. E., and Korc, M. (2000) A novel type I fibroblast growth factor receptor activates mitogenic signaling in the absence of detectable tyrosine phosphorylation of FRS2. *J. Biol. Chem.* **275,** 15933–15939.
12. Pastone, G., and Maher, P. (1996) Copper and calcium binding motifs in the extracellular domains of fibroblast growth factor receptors. *J. Biol. Chem.* **271,** 3343–3346.
13. Chaudhuri, M. M., Moscatelli, D., and Basilico, C. (1993) Involvement of the conserved acidic amino acid domain of FGF receptor 1 in ligand–receptor interaction. *J. Cell. Physiol.* **157,** 209–216.
14. Shimizu, A., Tada, K., Shukunami, C., Hiraki, Y., Kurokawa, T., Magane, N., and Kurokawa-Seo, M. (2000) A novel alternatively spliced fibroblast growth factor receptor 3 isoform lacking the acid box domain is expressed during chondrogenic differentiation of ATDC5 cells. *J. Biol. Chem.* **276,** 11031–11040.
15. Shukunami, C., Shigeno, C., Atsumi, T., Ishizeki, K., Suzuki, F., and Hiraki, Y. (1996) Chondrogenic differentiation of clonal mouse embryonic cell line ATDC5 *in vitro:* Differentiation-dependent gene expression of parathyroid hormone (PTH)/PTH-related peptide receptor. *J. Cell Biol.* **133,** 457–468.
16. Keegan, K., Meyer, S., and Hayman, M. J. (1991) Structural and biosynthetic characterization of the fibroblast growth factor receptor 3 (FGFR-3) protein. *Oncogene* **6,** 2229–2236.
17. Hynes, R. O. (1992) Integrins: Versatility, modulation, and signaling in cell adhesion. *Cell* **69,** 11–25.
18. Enomoto-Iwamoto, M., Iwamoto, M., Nakashima, K., Mukuda, Y., Boettiger, D., Pacifici, M., Kurisu, K., and Suzuki, F. (1997) Involvement of alpha5beta1 integrin in matrix interactions and proliferation of chondrocytes. *J. Bone Miner. Res.* **12,** 1124–1132.
19. Henderson, J. E., Naski, M. C., Aarts, M. M., Wang, D., Cheng, L., Goltsman, D., and Ornitz, D. M. (2000) Expression of FGFR3 with the G380R achondroplasia mutation inhibits proliferation and maturation of CFK2 chondrocytic cells. *J. Bone Miner. Res.* **15,** 155–165.
20. Huang, S., and Ingber, D. E. (1999) The structural and mechanical complexity of cell-growth control. *Nature Cell Biol.* **1,** E131–E138.
21. Sherr, C. J., and Roberts, J. M. (1995) Inhibitors of mammalian G1 cyclin-dependent kinases. *Genes Dev.* **9,** 1149–1163.
22. Spivak-Kroizman, T., Mohammadi, M., Hu, P., Jaye, M., Schlessinger, J., and Lax, I. (1994) Point mutation in the fibroblast growth factor receptor eliminates phosphatidylinositol hydrolysis without affecting neuronal differentiation of PC12 cells. *J. Biol. Chem.* **269,** 14419–14423.
23. Kouhara, H., Hadari, Y. R., Spivak-Kroizman, T., Schilling, T., Bar-Sagi, D., Lux, I., and Schlessinger, J. (1997) A lipid-anchored Grb2-binding protein that links FGF-receptor activation to the Ras/MAPK signaling pathway. *Cell* **89,** 693–702.
24. Ong, S. H., Guy, G. R., Hadari, Y. R., Luks S., Gotoh, N., Schlessinger, J., and Lax, I. (2000) FRS2 proteins recruit intracellular signaling pathways by binding to diverse targets on fibroblast growth factor and nerve growth factor receptors. *Mol. Cell. Biol.* **20,** 979–989.
25. Huang, S., Chen, C. S., and Ingber, D. E. (1998) Control of cyclin D1, p27(Kip1), and cell cycle progression in human capillary endothelial cells by cell shape and cytoskeletal tension. *Mol. Biol. Cell* **9,** 3179–3193.
26. Sewing, A., Wiseman, B., Lloyd, A. C., and Land, H. (1997) High-intensity Raf signal causes cell cycle arrest mediated by p21Cip1. *Mol. Cell. Biol.* **17,** 5588–5597.
27. Woods, D., Parry, D., Cherwinski, H., Bosh, E., Lees, E., and McMahon, M. (1997) Raf-induced proliferation or cell cycle arrest is determined by the level of Raf activity with arrest mediated by p21Cip1. *Mol. Cell. Biol.* **17,** 5598–5611.
28. Pumiglia, K. M., and Decker, S. J (1997) Cell cycle arrest mediated by the MEK/mitogen-activated protein kinase pathway. *Proc. Natl. Acad. Sci. USA* **94,** 448–452.
29. Hadari, Y. R., Kouhara, H., Lax, I., and Schlessinger, J. (1998) Binding of Shp2 tyrosine phosphatase to FRS2 is essential for fibroblast growth factor-induced PC12 cell differentiation. *Mol. Cell. Biol.* **18,** 3966–3973.
30. Das, D., Pintucci, G., and Stern, A. (2000) MAPK-dependent expression of p21(WAF) and p27(kip1) in PMA-induced differentiation of HL60 cells. *FEBS Lett.* **472,** 50–52.